Central European Journal of Energetic Materials
ISSN 1733-7178; e-ISSN 2353-1843

Cent. Eur. J. Energ. Mater. 2022, *19*(3): 326-359; DOI 10.22211/cejem/154975
Article is available in PDF-format, in colour, at:
https://ipo.lukasiewicz.gov.pl/wydawnictwa/cejem-woluminy/vol-19-nr-3/

Research paper

Rheological Properties of DNAN/HMX Melt-cast Explosives: Maximum Packing Density Calculation and Modified Viscosity Model

Jun-jiong Meng[1)], Yi-ming Luo[1)], Wei Wang[1)], Qiu-li Jiang[1)], Hong-xing Wang[1)], Fei-chao Miao[2,*)]

[1)] *Composite Explosive Research Department, Xi'an Modern Chemistry Research Institute, Xi'an 710065, China*
[2)] *School of Chemical Engineering, Anhui University of Science and Technology, Huainan 232001, China*
* *E-mail:* miaofeichao@qq.com

Abstract: The study of suspensions with high solid content and low viscosity has become a very active topic for melt-cast explosives, for both research and industry. Previous studies have described how the viscosity of high-solid-content suspensions can be decreased by optimizing the grade ratio, that is, increasing the particle packing density. This paper numerically simulates the maximum packing density (Φ_m) for different grade ratios at which the suspension viscosity approaches infinity, using the overlapping discrete element cluster method. According to this method, the shape of 1,3,5,7-tetranitro-1,3,5,7-tetrazocane (HMX) particles was modeled as a group of overlapping, rigidly connected hard spheres. The results showed that the numerical simulation value can be used as the real value of Φ_m for any grade ratio in engineering applications. The rheological properties of 2,4-dinitroanisole (DNAN)/HMX suspensions with various grade ratios of three HMX samples with different d_{50} values were investigated using a rotational viscometer over a range of mass solids content (φ = 20-75 wt.%) in the shear rate range of 0.1-100 s^{-1}. An empirical model incorporating the reduced solid content (Φ, equal to φ divided by Φ_m) and shear rate (γ) was modified to predict the relative viscosity of DNAN/HMX suspensions. This modified model has a strong

correlation with the experimental data and can be used to accurately predict the viscosity of DNAN/HMX suspensions. In addition, the applicability of different classical models to DNAN/HMX suspensions is discussed.

Keywords: 2,4-dinitroanisole, DNAN, grade ratio, maximum packing density, rheological properties, empirical model

Nomenclature

d_{50}	Diameter of coarse particles [mm]
DEM	Discrete Element Method
N	Constant used in the Nzihou model
n	A parameter of the shear rate (a power law index)
ODEC	Overlapping Discrete Element Cluster method
PSD	Particle size distribution
R	Regression coefficient
φ	Mass solids content [wt.%]
Φ	Reduced solid content (equal to φ divided by Φ_m)
Φ_m	Maximum packing density [g/cm^3]
γ	Shear rate [s^{-1}]
ζ	The grade ratio (the content of a particle class relative to other classes of particle)
λ	Size ratio (the ratio of the diameter (d_{50} in the present study) of coarse particles to that of fine particles of the next particle class)
$[\mu]$	Intrinsic viscosity of the matrix
μ_r	Relative viscosity
η	Viscosity of the suspension
η_s	Viscosity of the matrix
ρ	The ratio of the smallest to the largest ball
ρ_{app}	Apparent density of sample
ρ_p	Crystal density of HMX particles [g/cm^3]
σ	Standard deviation
θ	The maximum sphere-sphere intersection angle [°]

1 Introduction

The development of insensitive explosives has been the primary focus of research and development in many military organizations. In World War II, Germany was the first to use 2,4-dinitroanisole (DNAN) as the main charge

ingredient in Amatol 40:
– 50% DNAN,
– 35% ammonium nitrate (AN),
– 15% hexogen (RDX),
in the warheads of V-1 flying bombs [1]. However, because the energy performance of DNAN is relatively low, it was rarely used after World War II. With the development of insensitive ammunition in the United States and Europe, this typically insensitive energetic material has attracted renewed attention and is considered the best substitute for 2,4,6-trinitrotoluene (TNT) in the munitions field [2]. Nowadays, DNAN is used in a variety of formulations, notably PAX-21, IMX-101, and IMX-104 from the USA [3], ARX-4027, ARX-4028, and ARX-4029 from Australia [4], and MCX-6100 and MCX-8100 from Norway [5]. All these explosives have been shown to reduce the munitions' response to external threat stimuli in insensitive munitions testing while still meeting energy performance requirements.

Rheological properties are of particular importance for melt-cast explosives. To manufacture them, first the matrix explosive is completely melted. The solid particle explosive is then slowly added and evenly distributed in the liquid phase matrix using a suitable impeller, before the suspension is cast into the prepared projectile to solidify. During casting, the suspension should completely fill the shell. If the viscosity of the suspension is too large, it can cause shrinkage, pore formation, or other defects that reduces the charge quality and safety of the warhead. Therefore, the rheological properties of melt-cast explosives can indirectly influence the casting, formability, charge quality, and performance of the final product and have thus been a target of much recent and ongoing investigation.

Considerable work has been undertaken on the rheological properties of TNT-based melt-cast explosives with regards to the effect of solid content [6-8], particle size [9, 10], particle gradation [9, 11], particle morphology [12, 13], and temperature [14, 15]. However, very little information is available regarding the flow behavior of DNAN-based melt-cast explosives. Recently, the efflux viscosity and apparent viscosity of a few DNAN-based formulations, such as IMX-104 [16, 17], PAX-48 [16, 17], MCX-6100 and MCX-8100 [18], and ARX-4027 [19], were investigated and compared with Comp. B explosives. The effects on the rheological properties of five factors (solid content, particle size, particle gradation, temperature, and chemical additives) were thoroughly investigated by Meng *et al.* [20] and six factors (solid content, particle size, particle gradation, particle morphology, temperature, and chemical additives) of DNAN/1,3,5,7-tetranitro-1,3,5,7-tetrazocane (HMX) suspensions

were thoroughly investigated by Zhu *et al.* [21]. However, these studies can only provide guidance for formulation design and cannot predict the viscosity of DNAN/HMX explosives under different conditions.

According to the well-known Einstein equation (Equation 1) in a low-concentration suspension, there are fewer particles and no interactions between the particles.

$$\eta = (1 - [\mu]\ \varphi)\eta_s \tag{1}$$

where η is the viscosity of the suspension, $[\mu]$ is the intrinsic viscosity of the matrix, φ is the solid content, and η_s is the viscosity of the matrix. According to the literature, Φ is one of the most important parameters for studying the rheological properties. When φ exceeds about 20 wt.%, the interaction between particles begins to affect the viscosity. As the solid content continues to increase, the viscosity increases further until the solid content reaches the Φ_m. The value of Φ_m represents the best possible particle packing arrangement; once the solid particle content reaches this value, the apparent viscosity tends to infinity because the particles in the suspension can no longer be replaced [22]. Meanwhile, by changing the particle size distribution (PSD) from unimodal to bi-, tri-, tetra-, and finally to infinite-modal distribution, fine particles can fill the gaps between the coarse particles, and act as a lubricant. Thus the friction between the particles becomes smaller, and relative movement of the particles becomes increasingly easy. Φ_m can be increased to achieve viscosity optimization [23].

In the rigid sphere system, Φ_m can be calculated for different packing types with different PSDs [24]. However, in a non-spherical system, the irregular shape of the particles makes it very difficult to theoretically calculate Φ_m. To date, the most frequently used method to determine Φ_m is by means of a best-fit procedure to the rheological data for a given suspension [10]. The lack of an accurate computing method for Φ_m may limit the overall understanding of how particle characteristics affect rheological properties, which effectively restrains the further improvement of melt-cast explosive forming processes.

In this paper, we propose a possible means of computationally determining Φ_m and verify it by experiment. Furthermore, we also conducted 81 experiments to test the relative viscosity of trimodal DNAN/HMX suspensions in order to establish a model incorporating φ, Φ_m, power law index (n), $[\mu]$, and γ. This model enables the estimation of the viscosity of DNAN/HMX suspensions at any solid content and shear rate.

2 Materials and Test Methods

2.1 Samples

The DNAN used in this work was purchased from Hubei Dongfang Chemical Industry Group Co., Ltd. (Hubei, China) with purity 99.80% and used without further purification. It possessed a melting point and density of 94-96 °C and 1.52-1.54 g/cm^3, respectively. Three representative particle sizes of HMX were collected from different mesh sizes and designated as S-1, S-2, and S-3 (Gansu Yinguang Chemical Industry Group Co., Ltd., China).

A full factorial design was carried out for 9 grade ratios and 9 solid content fractions, resulting in 81 different test samples. In order to produce the 9 grade ratios, the S-3, S-2 and S-1 of HMX were mixed in the proportions (on a weight basis) of:

– 40:50:10 (G-1),
– 40:40:20 (G-2),
– 40:30:30 (G-3),
– 50:40:10 (G-4),
– 50:30:20 (G-5),
– 50:20:30 (G-6),
– 60:30:10 (G-7),
– 60:20:20 (G-8), and
– 60:10:30 (G-9).

The DNAN/HMX suspension contained 9 levels of HMX solid contents: 20, 30, 40, 50, 55, 60, 65, 70, and 75 wt.%.

The PSD of the starting samples were determined using a Mastersizer 2000M fitted with a dispersing unit Hydro 2000 MU (Malvern Instruments Ltd., Malvern, U.K.) and are plotted in Figure 1.

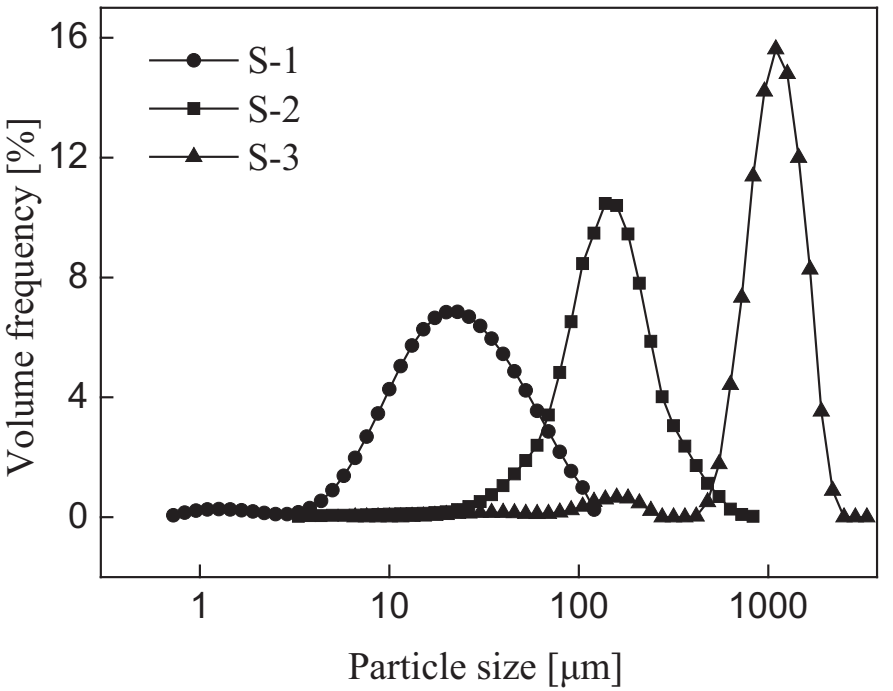

Figure 1. Particle size distribution of the three HMX samples

As shown in Figure 1, the d_{50} of the samples were found to be 24, 133 and 999 μm for S-1, S-2, and S-3, respectively. The PSD of the HMX samples conforms to a lognormal distribution, which can be expressed as Equation 2.

$$f(x) = \frac{1}{\sigma\sqrt{2\pi}} e^{-\frac{(x-\mu)^2}{2\sigma^2}} \tag{2}$$

where μ is the expected value (which determines the position of the normal distribution) and σ is the standard deviation (which determines the amplitude of the distribution). The HMX particle parameters μ and σ that are defined in Equation 1 are presented in Table 1.

Table 1. Fitting parameters of lognormal distribution

Sample	μ	σ	R^2
S-1	0.884	0.514	0.987
S-2	2.159	0.216	0.994
S-3	3.102	0.143	0.993

As shown in Table 1, the lognormal distribution was capable of a very good fit when simulating the PSD of different HMX samples. As the particle size increases, μ increases but σ decreases, indicating that the width of the PSD becomes smaller.

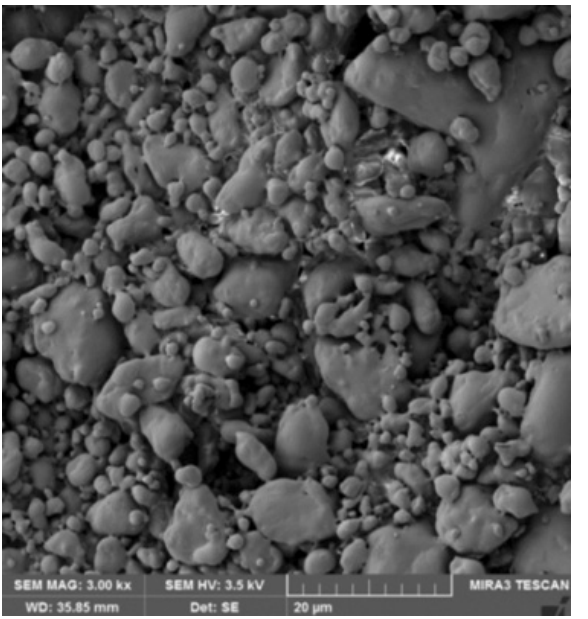

(a)

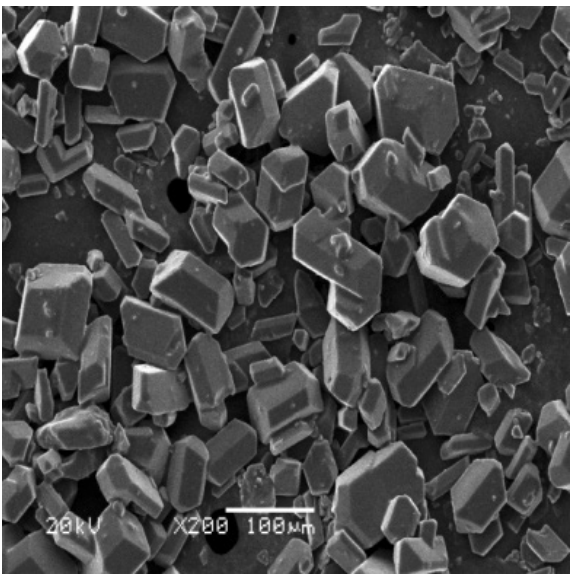

(b)

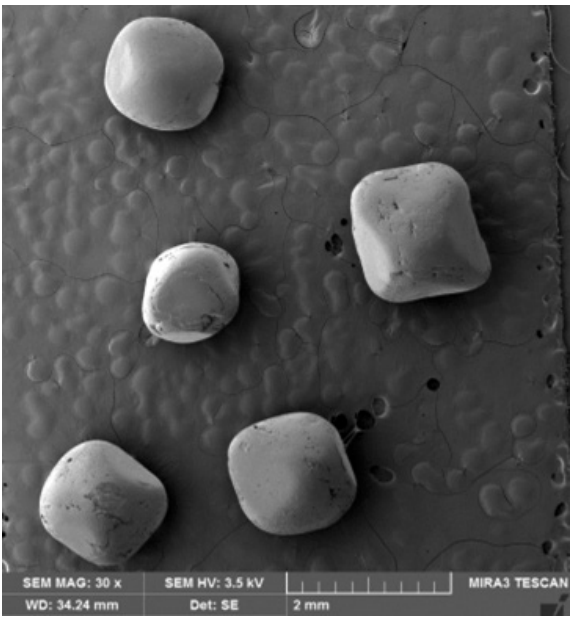

(c)

Figure 2. Morphological characterization of HMX samples of S-1 (a), S-2 (b), and S-3 (c)

Morphological analysis of typical fine (S-1), medium (S-2) and coarse (S-3) HMX particles was conducted using scanning electron microscopy (SEM, model MIRA3, TESCAN Brno, s.r.o., Czech Republic). As shown in Figure 2, S-1 (Figure 2(a)) has a large particle size dispersion and a complex crystal state, which was mainly irregularly spherical. S-2 (Figure 2(b)) was a polyhedron with dendrites on its surface. S-3 (Figure 2(c)) was a nearly spherical shape with regular morphology and a smooth surface without branching and cracking.

2.2 Measurement of viscosity

A rotational viscometer (model MCR302, Anton Paar GmbH, Graz, Austria) fitted with a CC27 concentric cylinder geometry was used to measure the viscosity of DNAN/HMX suspensions. The experimental data were recorded and processed using Rheoplus software (version 3.61). The shear rate was logarithmically ramped up from 0.1 to 100 s^{-1} in 101.2 s, and 19 data points were recorded. For each test, about 50 g of sample were placed in the concentric cylinder of the rheometer. The sample was heated internally until the end of the experiment by a PTD180 Peltier temperature controlling system, which can cover the temperature range of 0-180 °C. For the present study, viscosity measurements were performed at 105 °C. In order to reduce the experimental error, the viscosity of each sample was tested at least three times and the average value was taken.

2.3 Experimental test of maximum packing density

The maximum packing densities of different particle grade ratios were measured in a cylindrical container with an inner diameter of 5 cm and height of 10 cm. First, the samples were dried in vacuum for about 12 h, after which their mass was accurately weighed. Samples were then dropped into the container through a hopper over the top of the container. The dried sample in the container was vibrated on the shaker until the volume did not change, and the apparent volume in the container was calculated. Finally, the apparent density (ρ_{app}) was obtained by dividing the mass of the sample by its apparent volume, and the maximum packing density was calculated using Equation 3.

$$\phi_m = \frac{\rho_{app}}{\rho_p} \tag{3}$$

where ρ_{app} is the apparent density of the sample and ρ_p is the crystal density of HMX particles. In order to reduce the number of experiments and while ensuring the accuracy of the experiment, only the apparent density of the nine grade ratios were tested, with each sample tested three times.

3 Calculation of the Maximum Packing Density of a Trimodal PSD

3.1 Numerical modelling

The Discrete Element Method (DEM) is a numerical simulation method proposed by Cundall and Strack in 1979 to study discontinuous medium problems. They mainly used it to calculate how a large number of particles move under given conditions [25]. It has been successfully applied in mining engineering, geotechnical engineering, and other fields, and over the years it has attracted more and more attention in both engineering and academic circles.

To simplify the model, the default shape of the traditional DEM method was simple discs(two-dimensional) or spheres (three-dimensional). Particle materials with irregular shapes or large aspect ratios are very different from those simplified shapes, which limits the application of DEM numerical research to such materials. In order to obtain reliable results and improve the accuracy of numerical simulation, the actual shape of particles should be considered. In early research, researchers proposed a variety of non-circular particle profile modeling formulas, such as ellipse (sphere), polygon (body), hypersurface, and other irregular shapes. However, these methods still have some defects and cannot accurately simulate the shape of irregular particles [26, 27].

Ashmawy *et al*. [28] proposed an accurate two-dimensional Overlapping Discrete Element Cluster (ODEC) method to simulate the irregular shape of real particles. The core idea of ODEC technology was to overlap a series of two-dimensional discs in the outline of a particle shape, such that the final outer contour of the disc closely represented the shape of a particle. The advantage of ODEC was that the built-in particle clump algorithm excludes the contact between disks belonging to the same clump from iterative calculations, thus reducing the total amount of calculation.

The clump logic enables groups of particles to behave as a rigid body (Itasca 2008) approximating a non-spherical particle, but many discrete element softwares do not provide for any means to automatically create clumps. Taghavi [29] proposed a method for automatic creation of clumps approximating an arbitrary shape using an input triangular surface and two parameters describing the fidelity of the clump to the input surface. It relies on the properties of Delaunay tetrahedralization [30] to approximate the medial axis of an object. This method was implemented in a program called BubblePack [31] which automatically creates a clump and generates a list of ball locations and radii that can be read into discrete element software as a template for further replication.

3.2 Modelling of real particle shape

In this paper, the ODEC method was used to simulate the real shape of three-dimensional particles by clumping a certain number of overlapping spheres that were rigidly connected with each other. The following approach was used to build a clump while limiting the required number of balls:

(1) SEM was used to take a photograph of HMX particles in three directions (x, y, z), and extract the three-dimensional shape information of the particles. As an example, Figure 3 contains images for S-3 HMX particles.

(a)

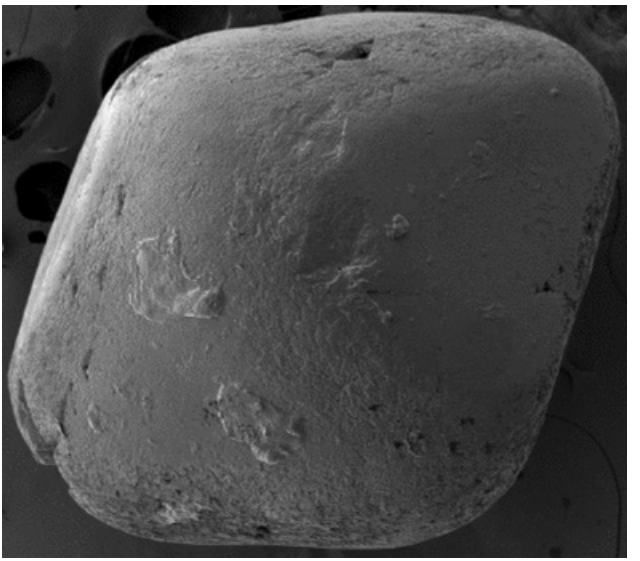

(b)

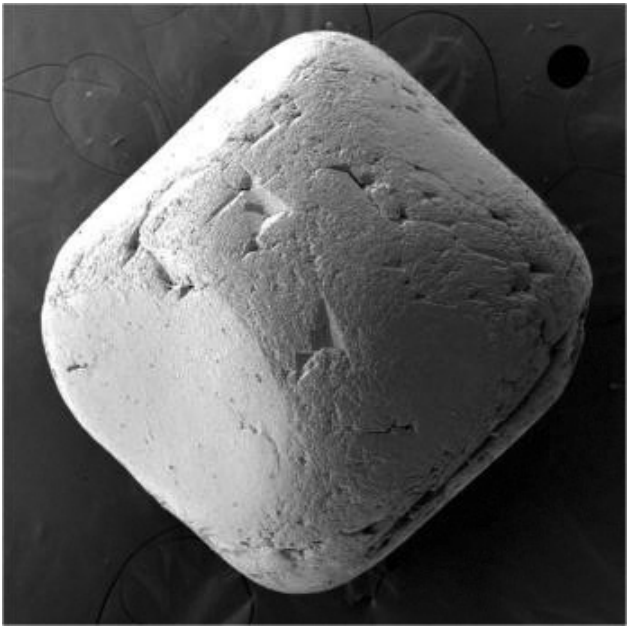

(c)

Figure 3. Three views of S-3 type HMX particles

(2) According to the three-dimensional information of particles, the particle shape was reconstructed in 3D modeling software, and an STL file was generated.

(3) Import the STL file, as shown in Figure 4. The initial surface mesh was optimized using the atomic force microscope (AFM) method to generate a triangular surface mesh, as shown in Figure 5. The volume mesh was divided using Delaunay triangulation using the bubble pack method algorithm, and the results are shown in Figure 6.

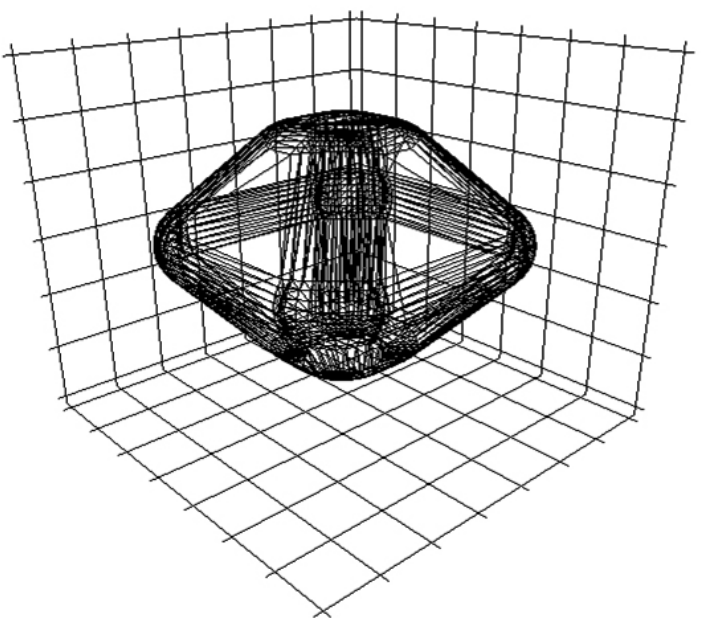

Figure 4. Particle morphology and initial surface mesh

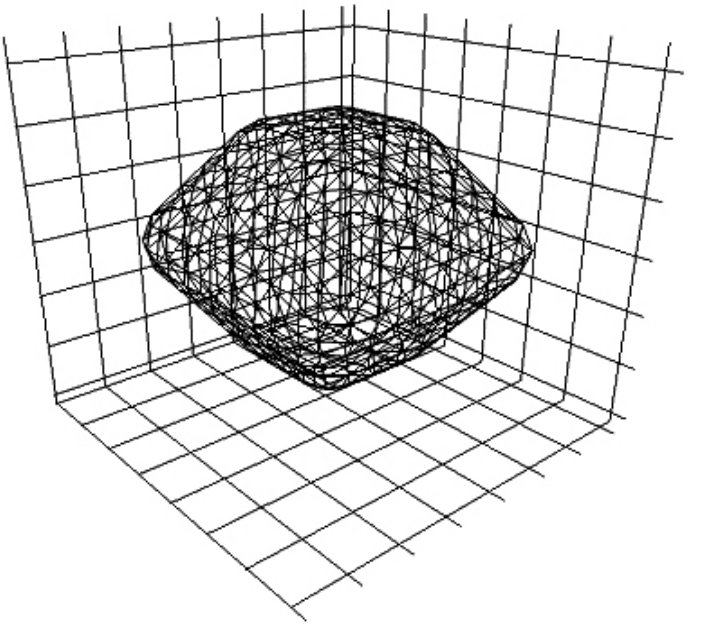

Figure 5. Optimized surface meshes

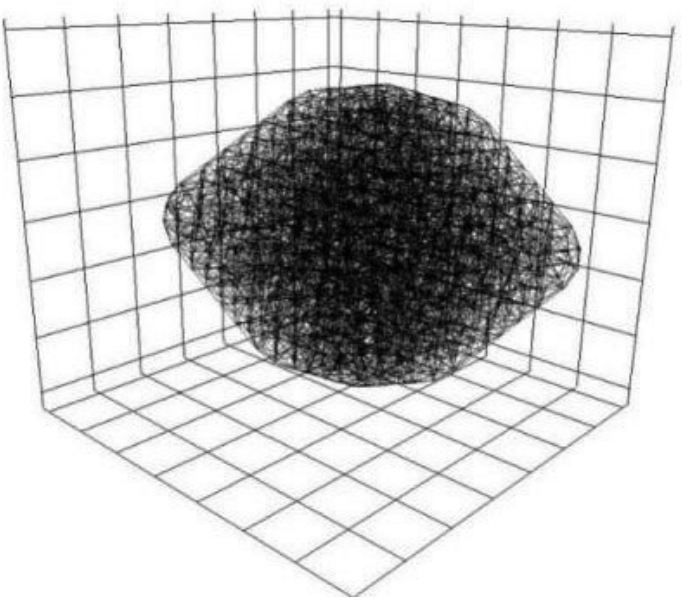

Figure 6. Volume meshes

(4) According to the Taghavi method, the ratio of the smallest to the largest ball (ρ), and the maximum sphere-sphere intersection angle (θ), are adjusted for automatic creation of clump blocks (see Figure 7). The adjustment process is shown in Figure 8. Based on the calculation ability and accuracy of the computer, $\rho = 0.3$ and $\theta = 160°$ were selected to generate a clump block for the calculation of Φ_m. A file was generated describing a clump template, as shown in Figure 9.

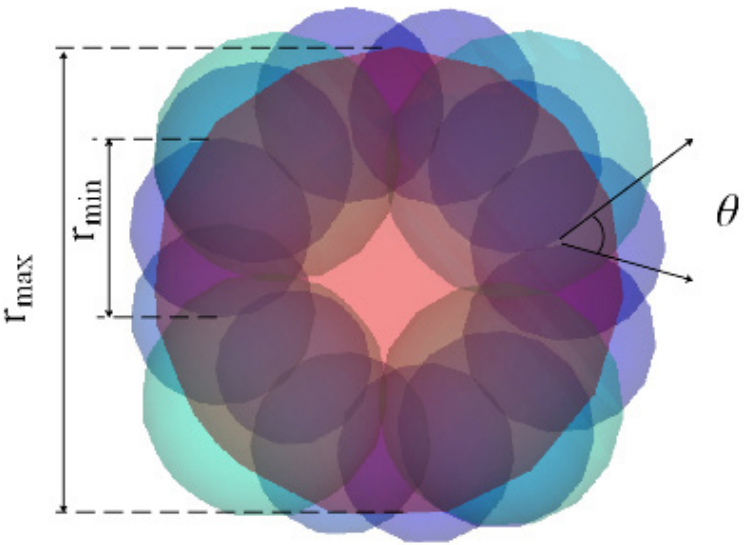

Figure 7. Two parameters determining the clump template of ρ and θ

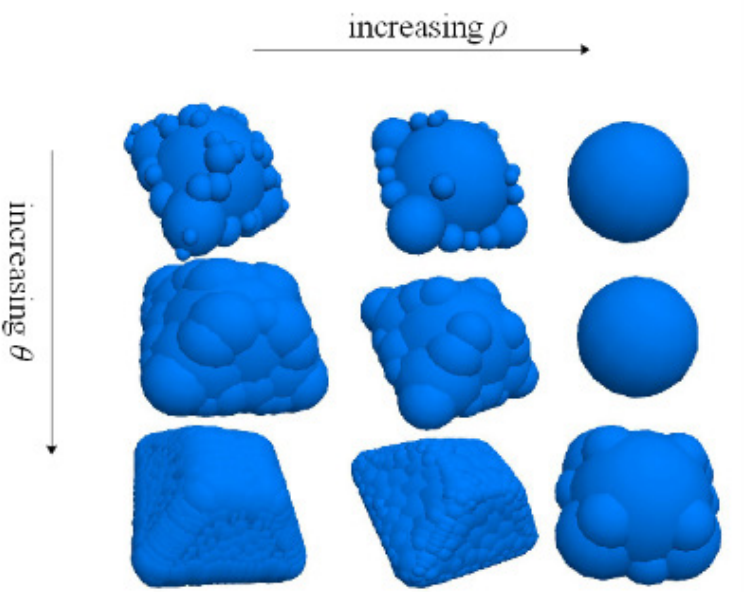

Figure 8. Influence of parameters ρ and θ on the shape of a clump

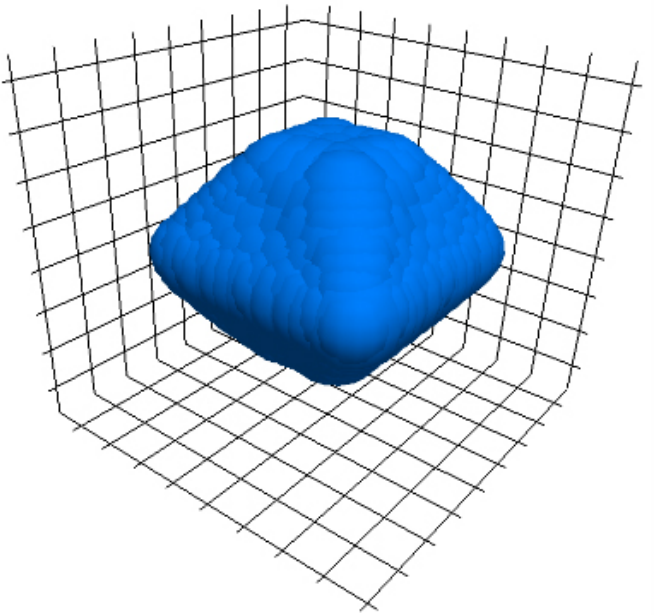

Figure 9. Clump block with $\rho = 0.3$ and $\theta = 160°$

3.3 Determination of Φ_m

In the actual accumulation system, S-1 had a large quantity of small particles with an almost spherical shape. To reduce the amount of calculation required, the particles are simplified to be spherical in the simulations. The S-2 particles were larger and polyhedral, while the S-3 particles were the largest and had an ellipsoidal shape. These two particle shapes have a major influence on the packing density, and modelling must effectively consider this in order to obtain accurate calculation results.

A suitable calculation and solution area were established using a cylindrical container as the boundary condition for particle accumulation. The diameter and height of this container were 5 and 10 cm, respectively. According to the previously determined shape, particle size distribution, and particle grading ratio, a random loose accumulation structure is formed in the cylinder. Gravity is then enabled to allow the clump blocks and particles to settle freely, with particles colliding with each other and the container wall. Eventually, the system reached a stable and close packing state, as shown in Figure 10, at which point the maximum packing density was calculated.

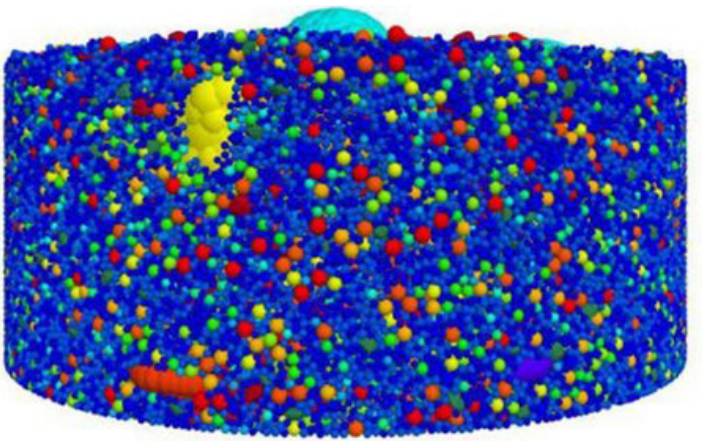

(a)

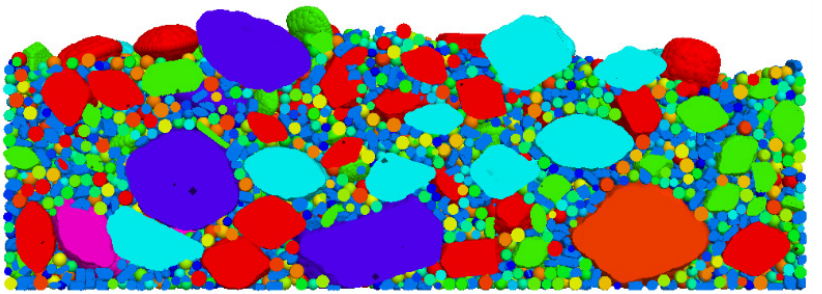

(b)

Figure 10. Close packing under gravity of exterior (a) and longitudinal (b) sections

4 Results and Discussion

4.1 Effect of grade ratio on Φ_m

Figure 11 presents the effect of the grade ratios on the Φ_m, based on the ODEC method. As shown in Figure 11, the influence of S-3 and S-1 fractions on the Φ_m was parabolic. Φ_m gradually increased as the content of coarse (S-3) particles in the HMX increased from 0 to 53% but decreased as the S-3 content increased beyond 53%. The maximum Φ_m achieved was 0.8401, using a mixture of 20 wt.% fine particles (S-1), 27 wt.% medium particles (S-2), and 53 wt.% coarse particles (S-3).

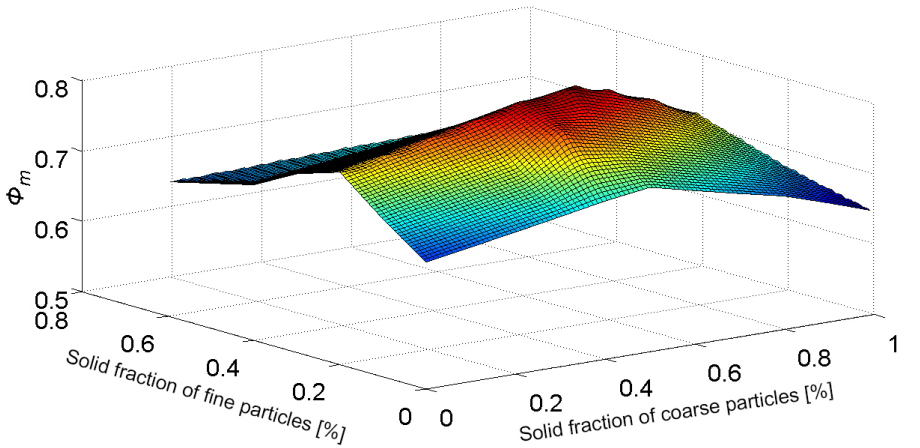

Figure 11. Three-dimensional plot of Φ_m

Table 2 shows Φ_m for the nine grade ratios described earlier, obtained using both experimental tests and numerical calculations. It can be seen from Table 2 that both the experimental tests and the numerical calculations found their maximum Φ_m values when the grade ratio (S-3:S-2:S-1) was 50:30:20 (*i.e.* G-5). Moreover, the Φ_m of the experimental tests were close to (although slightly lower than) the numerical calculations. This is likely because the numerical calculations were not comprehensive enough to perfectly reproduce the particle shapes, leading to higher values of Φ_m. However, the difference between numerical calculations and experimental tests was less than 4%, which is close enough that the numerically calculated value of Φ_m can be used in engineering applications.

Table 2. Φ_m of the different grade ratios used in this study

Sample	Grade ratio (S-3:S-2:S-1)	Φ_m	
		Experimental test	Numerical calculation
G-1	40:50:10	0.7932	0.8044
G-2	40:40:20	0.8261	0.8303
G-3	40:30:30	0.7766	0.7827
G-4	50:40:10	0.7752	0.7859
G-5	50:30:20	0.8293	0.8377
G-6	50:20:30	0.7882	0.7969
G-7	60:30:10	0.7577	0.7683
G-8	60:20:20	0.8147	0.8270
G-9	60:10:30	0.7981	0.8063

4.2 Rheological behavior of the DNAN/HMX suspension

The variation of relative viscosity for different grade ratios for 40 and 65 wt.% solid content is shown in Figure 12. At constant solid content, the relative viscosity decreased with increasing shear rate, causing a shear-thinning behavior. This is mainly because the increase in shear rate destroys the internal network structure of the suspension. As a result, the particles align along the shear direction and the resistance to deformation is poor. As the shear rate continues to increase, the apparent viscosity curve of the suspension tends to be flat. This indicates that the interaction between particles is destroyed in this range of shear rates. The particles tend to be dispersed, the interaction between particles is weak, and the viscosity of the suspension is reduced [32].

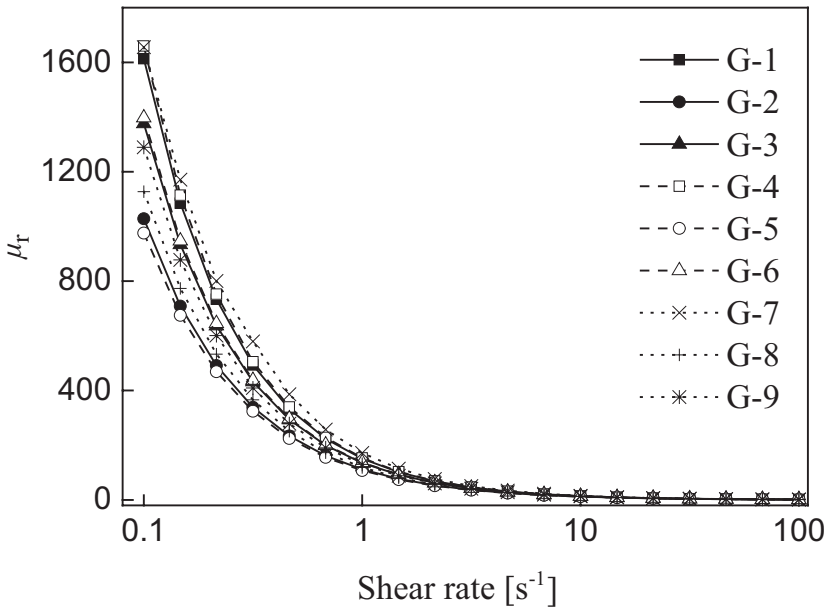

(a)

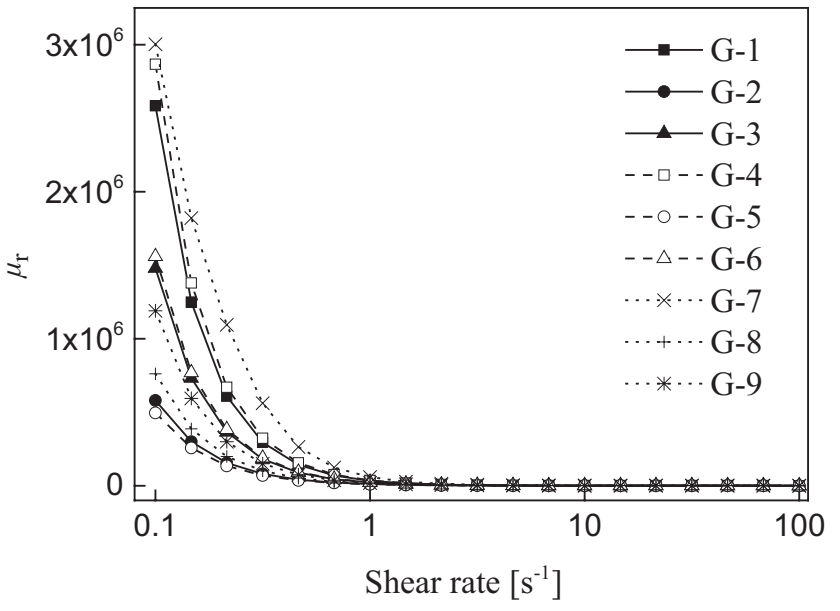

(b)

Figure 12. Variation of the relative viscosity versus shear rate: 40 (a) and 65 wt.% (b)

The viscosity of DNAN/HMX suspensions with higher solid content also increased with increasing solid content, as shown in Figure 12; the same trend has been generally observed previously in TNT/RDX suspensions [6]. With low-solid-content DNAN/HMX suspensions, there is a greater amount of molten DNAN between the HMX particles, and hence the friction between the particles is very small. Therefore, the resistance induced by solid particles during stirring is small and the viscosity is relatively low. As the solid content is gradually increased, the relative movement of the particles becomes more difficult due to the reduction in volume of the continuous phase and decreased spacing between particles. Therefore, stirring resistance increases due to the frequent collisions and friction between the solid particles, leading to decreased mobility of the suspension and higher viscosity.

Results also indicate obvious differences between the rheological properties for different grade ratios. In general, HMX with 20 wt.% fine particles, 30 wt.% medium particles, and 50 wt.% coarse particles (G-5) displays a lower relative viscosity than the other grade ratios. Therefore, Φ_m was maximized and the suspension viscosity was minimized when G-5 was used for the formulation.

It is established that Φ_m is affected by two key parameters [33]:

– the size ratio (λ), the ratio of the diameter (d_{50} in the present study) of coarse particles to that of fine particles of the next particle class, and
– the grade ratio (ζ), the content of a particle class relative to other classes of particle.

The viscosity of the suspension can be reduced by adding small particles with appropriate size into the suspension containing large particles. This is because the small particles in the pores between the large particles can act as a lubricant for the flow of the large particles, thus reducing the viscosity of the whole system [34]. McGeary [35], Lee [36], and Metzner [37] found the viscosity to be at minimum when λ was greater than 7, *i.e.* if the diameter of coarse particles was at least 7 times greater than that of fine particles of the next particle class. This is valid for bi-, tri-, and tetramodal PSDs. In the present study, the ratios $R_{S\text{-}1}/R_{S\text{-}2} = 7.5$ and $R_{S\text{-}2}/R_{S\text{-}3} = 5.6$ were close to the optimum ratio of 7 found in previous studies of viscosity.

Farris [23] showed that, at 64% solid content, there was an optimal grade ratio between fine and coarse particles that could maximize Φ_m and minimize viscosity. For the trimodal PSD, the optimum ratio was 22.5%, 32% and 45.5% for fine, medium, and coarse particles, respectively. This is close to the optimal ratio determined by this study's numerical calculation results (20 wt.% fine particles, 27 wt.% medium particles and 53 wt.% coarse particles).

4.3 Modelling of viscosity measurement

Figure 13 shows the relationship between relative viscosity and solid content for different grade ratios when the shear rate is 10 s^{-1}. As shown in Figure 13, when the solid content was less than approximately 60 wt.%, the particle grade ratio exhibited a negligible effect on suspension viscosity. However, for solid contents greater than 60 wt.%, the relative viscosity of the DNAN/HMX suspensions increased exponentially with solid content.

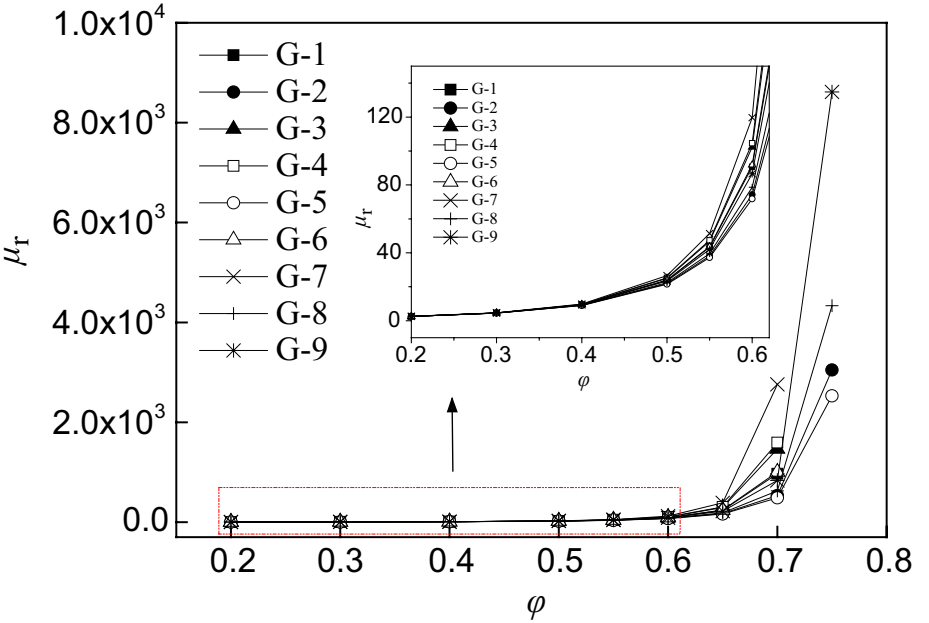

Figure 13. Relationship between relative viscosity and solid content of different grade ratios at a shear rate of 10 s^{-1}

All the curves showed that the relative viscosity increased slowly and monotonically with the solid content until a certain critical point, beyond which a small increment of solid content caused a significant increase in relative viscosity. Obviously, the solid content at which the relative viscosity begins to increase to infinity may be directly related to (or close to) Φ_m at this grade ratio. This conclusion was also confirmed by other researchers for different suspension systems [37].

As mentioned above, the main purposes of this study was to correlate the variation of relative viscosity with solid content and shear rate and to establish an applicable model to accurately predict the viscosity of DNAN/HMX suspensions.

It can be seen from Figure 13 that the effect of solid content on the relative viscosity is the same even when using different grade ratios. However, the relationship cannot be expressed exactly by the same model. In order to obtain a general empirical model of relative viscosity and solid content, this work introduces the concept of reduced solid content (Equation 4). Using Equation 4, the abscissa of each curve in Figure 13 is divided by its respective maximum packing density, and these results are shown in Figure 14.

$$\Phi = \varphi/\Phi_m \tag{4}$$

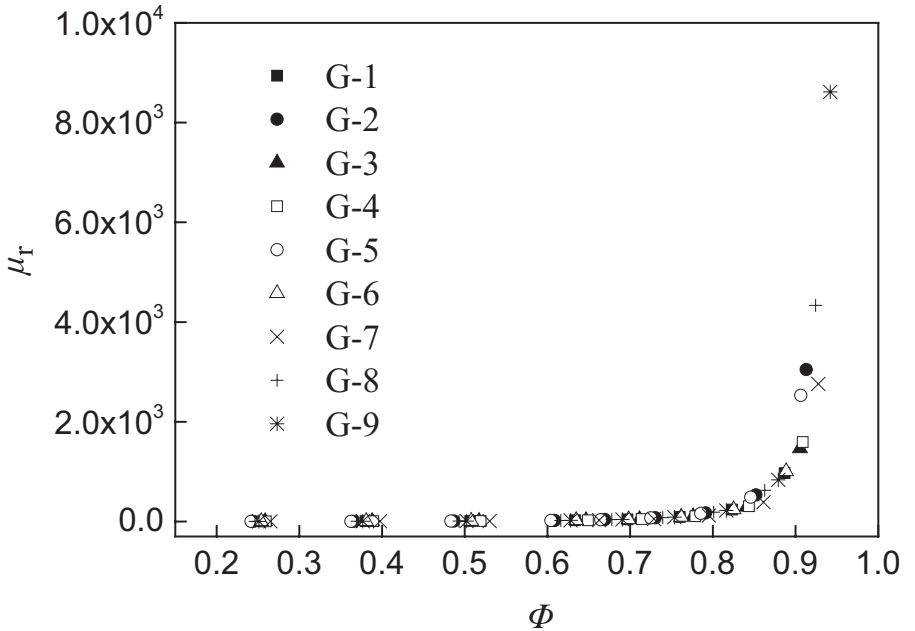

Figure 14. Relative viscosity of suspensions versus reduced solid content of different grade ratios

These results show that the concept of Φ has significant potential use in describing the variation of relative viscosity with different grade ratios. As shown in Figure 14, the relative viscosity of different grade ratios can be fitted with the same exponential function.

Various theoretical and empirical models have been developed to estimate the viscosity of suspensions, such as the Maron and Pierce model [38] (Equation 5), the Eiler model [39] (Equation 6), the Krieger-Dougherty model [40] (Equation 7), the Chong model [41] (Equation 8) and the Nzihou model [42] (Equation 9).

$$\mu_{\mathrm{r}} = \left(1 - \frac{\phi}{\phi_m}\right)^{-2} \tag{5}$$

$$\mu_r = \left(1 + 1.25\frac{\phi}{1-\frac{\phi}{\phi_m}}\right)^2 \tag{6}$$

$$\mu_r = \left(1 - \frac{\phi}{\phi_m}\right)^{-A\phi_m} \tag{7}$$

$$\mu_r = \left[1 + 0.75\frac{\frac{\phi}{\phi_m}}{\left(1-\frac{\phi}{\phi_m}\right)}\right]^2 \tag{8}$$

$$\mu_r = \left[1 + \frac{D}{\gamma^n}\frac{\frac{\phi}{\phi_m}}{\left(1-\frac{\phi}{\phi_m}\right)}\right]^B \tag{9}$$

The Nzihou model given in Equation 9 shows the relationship between relative viscosity and shear rate and solid content, which is useful for the present analysis. Based on the fact that relative viscosity and reduced solid content can be described by a single curve, the model needs to be further modified. Therefore, a modified three-parameter model is proposed as a function of reduced solid content and shear rate. This model is expressed as Equation 10. This equation comprehensively takes into account the Φ, γ, n and $[\mu]$ parameters.

$$\mu_r = \left[1 + \frac{[\mu]}{\gamma^n}\frac{\Phi}{(1-\Phi)}\right]^N \tag{10}$$

where N is a suspension-dependent parameter. Under high shear rate conditions, the value of the index N in most of the above models is taken as 2. However, this value needs to be determined experimentally in the case of low to medium shear rates [43]. The physical mean of the constants N used in the Nzihou model were taken from the Krieger-Dougherty model (Equation 7), and the results are presented in Table 3. It can be seen that the value of N for all grade ratios is between 3.23541 and 5.04861, which is greater than the value of 2 used in the Maron and Pierce, Eiler, and Chong models. The average value of N for different grade ratios was 4.0087, which suggests that the model can use a constant value of 4 to replace N.

Table 3. *N* for the Krieger-Dougherty model

Grade ratio (S-3:S-2:S-1)	*N*	Regression coefficient (*R*)
40:50:10	4.07594	0.9999
40:40:20	5.04861	0.9868
40:30:30	4.09696	0.9911
50:40:10	3.23541	0.9962
50:30:20	4.45146	0.9975
50:20:30	3.36945	0.9917
60:30:10	3.71560	0.9994
60:20:20	4.60648	0.9940
60:10:30	3.47872	0.9955

The limiting value of $(\mu_r - 1)/\phi$ at low concentrations is called the intrinsic viscosity [44]. It is often represented by $[\mu]$. For hard spherical particles, Einstein's equation suggests an intrinsic viscosity $[\mu]$ of 2.5, and this value has been applied in some of the above models. This paper also adopts $[\mu] = 2.5$. By replacing the adjustable parameters N and $[\mu]$ in Equation 10 with constant values of 4 and 2.5, respectively, the following modified model is obtained (Equation 11).

$$\mu_r = \left[1 + \frac{2.5}{\gamma^n}\frac{\Phi}{(1-\Phi)}\right]^4 \tag{11}$$

The power law parameter n of the shear rate is according to the Casson model (Equation 12), which is used to describe yield stress materials with $[\mu]$ as a constant. At sufficiently high shear rate, the value of $n = 0.5$ and at low shear rate, the n values must be determined separately.

$$\tau^{0.5} = \tau_c^{0.5} + (\mu_c\dot{\gamma})^{0.5} \tag{12}$$

The experimental data in Figure 14 can then be fitted to the modified model to obtain the power law parameter n. The resulting n parameter and the corresponding R are 0.67 and 0.9959, respectively. Figure 15 compares this proposed modified model with the experimental results of this study. As indicated by Figure 15, Equation 11 can accurately predict the experimental data when the shear rate is 10 s^{-1}.

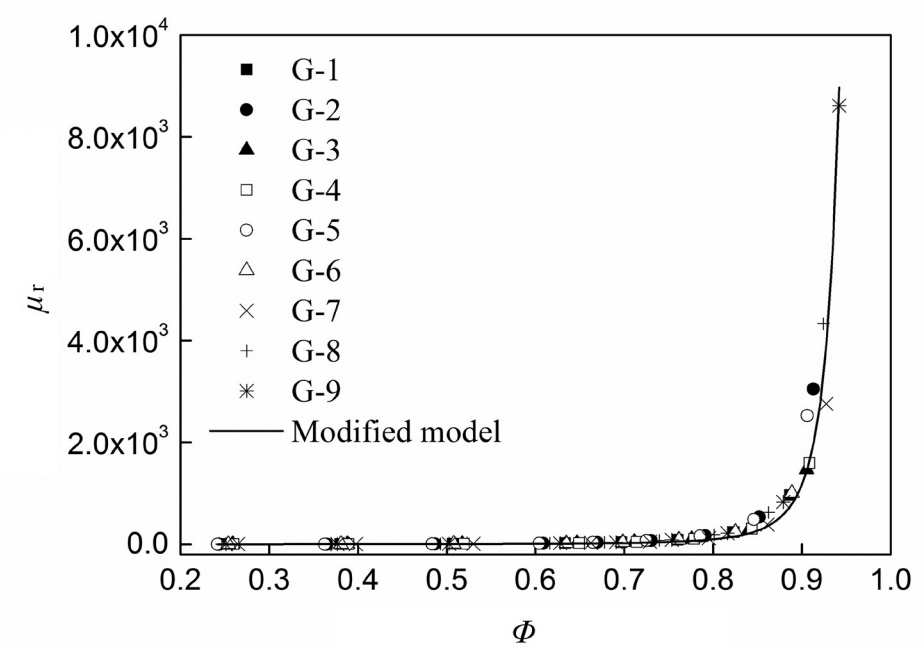

Figure 15. Comparison between the modified model and experimental results at shear rate of 10 s^{-1}

Therefore, the following model is obtained for predicting the relative viscosity of DNAN/HMX suspensions (Equation 13).

$$\begin{cases} \mu_r = \left[1 + \frac{2.5}{\gamma^{0.67}} \frac{\Phi}{(1-\Phi)}\right]^4 \\ \Phi = \frac{\phi}{\phi_m} \end{cases} \tag{13}$$

In order to evaluate the accuracy of Equation 12, the experimental data are compared with the predicted values of the modified model at shear rates of 100, 1 and 0.1 s^{-1}. The results are shown in Figure 16. The corresponding regression coefficients of these curves are 0.9961, 0.9959, and 0.9923, respectively, indicating that the modified model can accurately predict the viscosity of DNAN/HMX suspension systems at different shear rates.

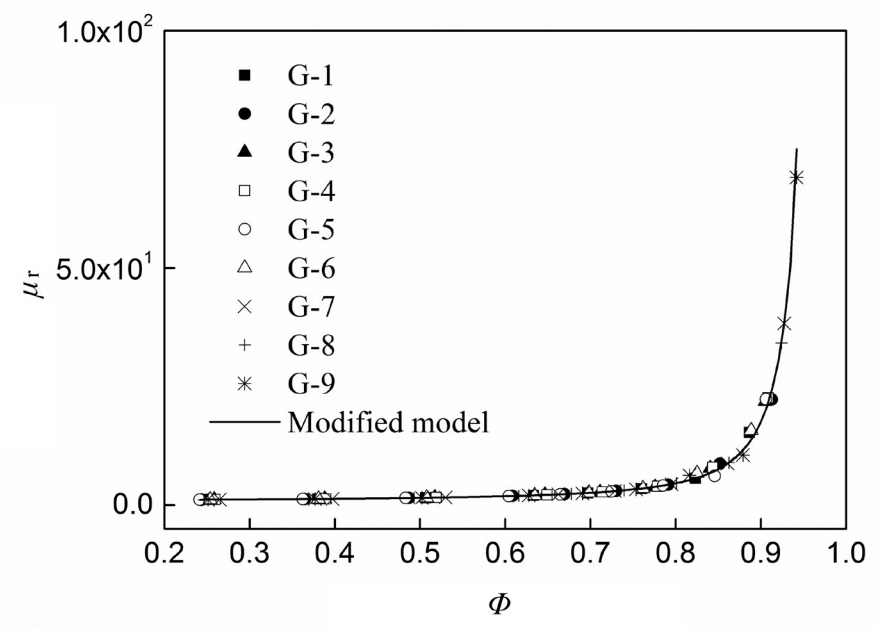

(a)

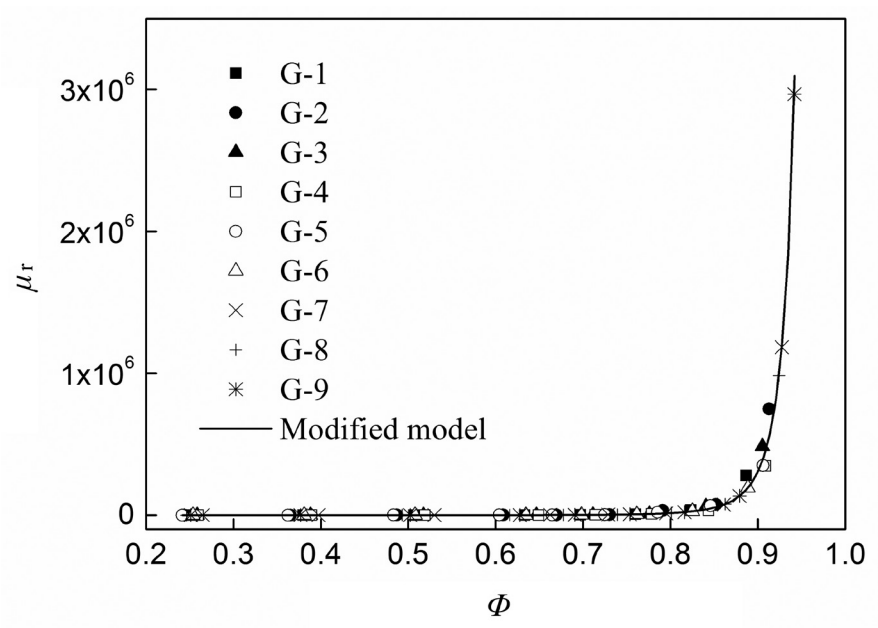

(b)

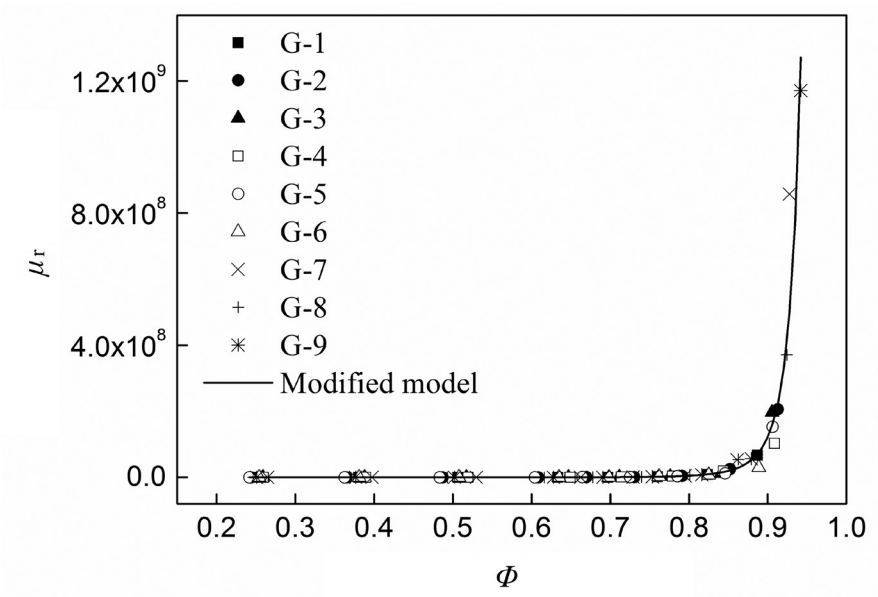

(c)

Figure 16. Comparison between the modified model and experimental data at different shear rates of 100 (a), 1 (b) and 0.1 (c) s^{-1}

In order to further check the performance and validity of the modified model, the experimental data of the G-5 DNAN/HMX suspension studied in this work were fitted using the empirical and theoretical models reported in the literature at different shear rates of 1, 10 and 100 s^{-1} in the range of 20 to 75 wt.% solid content. These models include the empirical model mentioned above, the Eiler model (Equation 6), the Krieger-Dougherty model (Equation 7), the Chong model (Equation 8), and the theoretical model proposed by Maron and Pierce (Equation 5). The results are displayed in Figure 17 and show that, compared with other models, the modified model proposed in this paper correlates better with the experimental data than the other models. Therefore, the model proposed in this work is most suitable for analysis of DNAN/HMX suspensions.

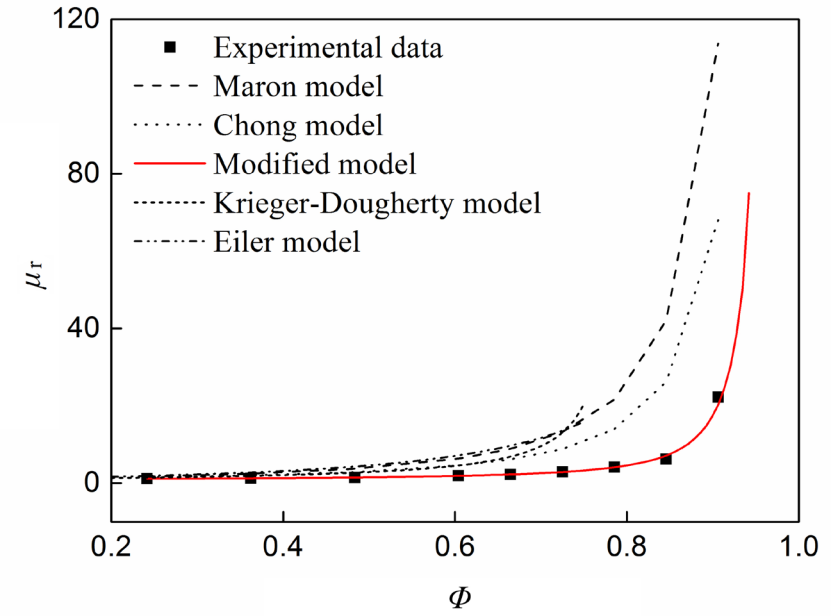

(a)

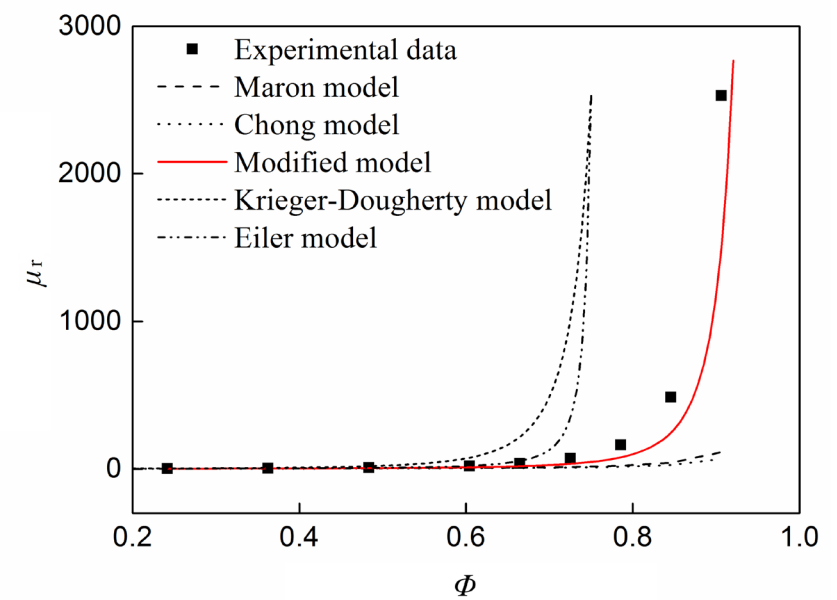

(b)

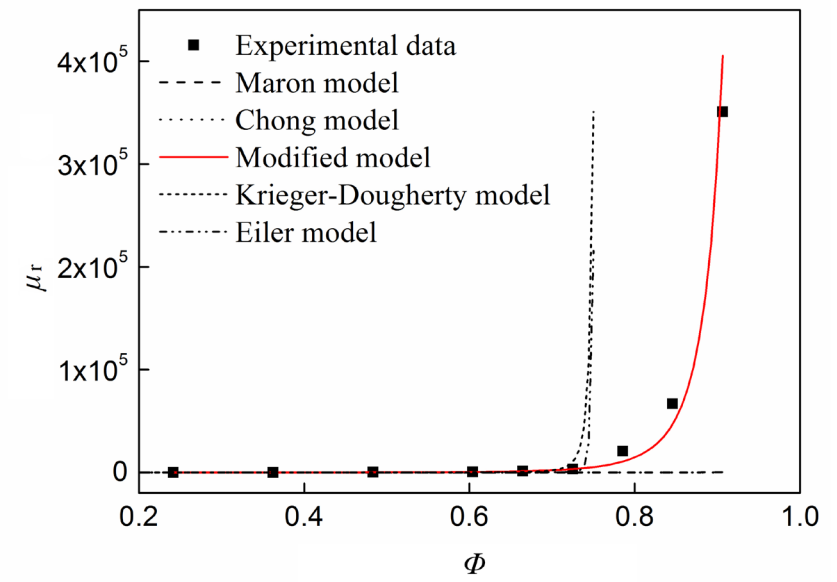

(c)

Figure 17. Comparison between the modified model and other models for G-5 at different shear rates of 100 (a), 1 (b) and 0.1 (c) s^{-1}

5 Conclusions

- It is well known that particle gradation can reduce the viscosity of suspension by changing the particle filling so that the fine particles can fill the gaps between the coarse particles. However, in order to make this information useful to the engineering applications of melt-cast explosives, it is necessary to calculate the Φ_m of DNAN/HMX suspensions with different grade ratios. In this study, we successfully developed an ODEM method to calculate the Φ_m of a trimodal PSD with different grade ratios. Based on the results of experiments in this study, it is possible to estimate the Φ_m for a trimodal PSD system of HMX. From this method, it was found that a ratio of20 wt.% fine particles, 27 wt.% medium particles, and 53 wt.% coarse particles provides the maximum Φ_m of 0.8401.
- The effect of solid particles on the relative viscosity of DNAN/HMX suspension was revealed by viscosity measurement. Experimental results indicate that the relative viscosity of suspensions is highly sensitive to the solid content and grade ratio. When the solid content is less than 60 wt.%,

the effect of the grade ratio on the apparent viscosity of the DNAN/HMX suspension is negligible. When the solid content is more than 60 wt.%, the grade ratio of HMX particles has a great influence on the relative viscosity of the DNAN/HMX suspension. In the nine grade ratios examined in this study, G-5 (S-3:S-2:S-1 = 50:30:20) achieved the greatest Φ_m and the lowest viscosity.

- A modified model based on the Nzihou model was proposed by comparing the experimental data with various existing models of concentrated suspensions. The proposed model relates the relative viscosity of the DNAN/HMX suspension to the shear rate and reduced solid content, in the form of $\mu_r = \left[1 + \frac{2.5}{\gamma^{0.67}} \frac{\Phi}{(1-\Phi)}\right]^4$. Further analysis shows that this model can accurately predict corresponding experimental data very well at different shear rates.
- In summary, the numerical calculation presented here for Φ_m and the modified model can be used to evaluate the process parameters for designing high solid content, low viscosity DNAN/HMX suspension explosives.

Acknowledgements

The authors would like to acknowledge National Natural Science Foundation of China (Grant No. 12002266) for providing funds for conducting the experiments.

References

[1] Ravi, P.; Badgujar, D.M.; Gore, G.M.; Tewari, S.P; Sikder, A.K. Review on Melt Cast Explosives. *Propellants Explos. Pyrotech.* **2011**, *36*(5): 393-403; DOI: 10.1002/prep.201100047.

[2] Boddu, V.M.; Abburi, K.; Maloney, S.W.; Damavarapu, R. Thermophysical Properties of an Insensitive Munitions Compound, 2, 4-Dinitroanisole. *J. Chem. Eng. Data.* **2008**, *53*(5): 1120-1125; DOI: 10.1021/je7006764.

[3] Taylor, S.; Ringelberg, D.B.; Dontsova, K.; Daghlian, C.P.; Walsh, M.E.; Walsh, M.R. Insights Into the Dissolution and the Three-dimensional Structure of Insensitive Munitions Formulations. *Chemosphere* **2013**, *93*(9): 1782-1788; DOI: 10.1016/j.chemosphere.2013.06.011.

[4] Provatas, A.; Wall, C. Ageing of Australian DNAN Based Melt-cast Insensitive Explosives. *Propellants Explos. Pyrotech.* **2016**, 4*1*(3): 555-561; DOI: 10.1002/prep.201500315.

[5] Nevstad, G.O. *Fragmentation of 40 mm Shell with 6 Different Compositions –4*

melt Cast and 2 Press Filled. Norwegian Defence Research Establishment, Report FFI-rapport-2015/02324, **2015**.

[6] Xu, G.G.; Xu, J.P. Rheological Properties of TNT/RDX Suspensions. (in Chinese) *Acta Armamentarii* **1991**, *2*: 71-74.

[7] Brousseau, P.; Thiboutot, S.; Ampleman, G. Behaviour of CL-20 in TNT-based Explosives. Proc. *38th Int. Annu. Conf. Fraunhofer ICT*, Karlsruhe, Germany, **2007**.

[8] Joshi, V.S.; Vadali, S.; Wasnik, R.D.; Jangid, S.K.; Maurya, M. Studies on Rheological Properties and Process Parameters of TNT Based Castable High Explosive Compositions. *Sci. Technol. Energ. Mater.* **2017**, *78*(4): 87-92.

[9] Singh, B.; Kaushik, D.R. Spheroidization of RDX and Its Effect on the Pourability of RDX/TNT Slurries. *Def. Sci. J.* **1989**, *39*(1): 95-98.

[10] Guillemin, J.P.; Brunet, L.; Bonnefoy, O.; Thomas, G. A Flow Time Model for Melt-cast Insensitive Explosive Process. *Propellants Explos. Pyrotech.* **2007**, *32*(3): 261-266; DOI: 10.1002/prep.200700028.

[11] Billon, H.H.; Parry, M.A. *The Viscosity of TATB Types A and B Suspensions in Molten TNT: General Characteristics*. Australia Materials Research Labs Ascot Vale, Report MRL-TR-91-24, **1991**.

[12] Guillemin, J.P.; Menard, Y.; Brunet, L.; Bonnefoy, O.; Thomas, G. Development of a New Mixing Rheometer for Studying Rheological Behaviour of Concentrated Energetic Suspensions. *J. Non-Newtonian Fluid Mech.* **2008**, *151*(1-3): 136-144; DOI: 10.1016/j.jnnfm.2007.12.007.

[13] Sarangapani, R.; Ramavat, V.; Reddy, S.; Subramanian, P.; Sikder, A.K. Rheology Studies of NTO-TNT Based Melt-cast Dispersions and Influence of Particle-dispersant Interactions. *Powder Technol.* **2015**, *273*: 118-124; DOI: 10.1016/j.powtec.2014.12.013.

[14] Parry, M.A.; Billon, H.H. A Note on the Coefficient of Viscosity of Pure Molten 2,4,6-Trinitrotoluene (TNT). *Rheol. Acta.* **1988**, *27*(6): 661-663.

[15] Zerkle, D.K.; Núñez, M.P.; Zucker, J.M. Molten Composition B Viscosity at Elevated Temperature. *J. Energ. Mater.* **2016**, *34*(4): 368-383; DOI: 10.1080/07370652.2015.1102179.

[16] Pelletier, P.; Laroche, I.; Lavigne, D.; Cantin, F.; Brousseau, P.; Fung, V. Processing Studies of DNAN Based Melt-pour Explosive Formulations. *Proc. Insensitive Munitions and Energetic Materials Technology Symp.*, Tucson, AZ, USA, **2009**.

[17] Fung, V.; Ervin, M.; Alexander, B.; Patel, C.; Samuels, P. Development and Manufacture of an Insensitive Composition B Replacement Explosive IMX-104 for Mortar Applications. *Proc. Insensitive Munitions and Energetic Materials Technology Symp.*, Munich, Germany, **2010**.

[18] Johansen, Ø.H.; Nevstad, G.O.; Gjersøe, R.; Berg, A.; Granby, T.; Ødegaard, M. Insensitive Munitions-development and Qualification of New Melt-cast Formulations. *Proc. Insensitive Munitions and Energetic Materials Technology Symp.*, Nashville, TN, USA, **2016**.

[19] Davies, P.J.; Provatas, A. *Characterisation of 2,4-Dinitroanisole: An Ingredient for Use in Low Sensitivity Melt Cast Formulations*. Australia Defense Science and

Technology Organization, Report DSTO-TR-1904, **2006**.
[20] Meng, J.J.; Zhou, L.; Jin, D.Y.; Cao, S.T.; Wang, Q.H. Rheological Properties of DNAN/HMX Melt-cast Explosives. *Chin. J. Energ. Mater.* **2018**, *26*(8): 677-685.
[21] Zhu, D.L; Zhou, L.; Zhang, X.R. Rheological Behavior of DNAN/HMX Melt-Cast Explosives. *Propellants Explos. Pyrotech.* **2019**, *44*(12): 1583-1589; DOI: 10.1002/prep.201900117.
[22] Senapati, P.K.; Mishra, B.K.; Parida, A. Modeling of Viscosity for Power Plant Ash Slurry at Higher Concentrations: Effect of Solids Volume Fraction, Particle Size and Hydrodynamic Interactions. *Powder Technol.* **2010**, *197*(1-2): 1-8; DOI: 10.1016/j.powtec.2009.07.005.
[23] Farris, R.J. Prediction of the Viscosity of Multimodal Suspensions from Unimodal Viscosity Data. *Trans. Soc. Rheol.* **1968**, *12*(1): 281-301.
[24] Larrard, F.D.; Sedran, T. Mixture-proportioning of High-performance Concrete. *Cem. Concr. Res.* **2002**, *32*(11): 1699-1704; DOI: 10.1016/S0008-8846(02)00861-X.
[25] Cundall, P.A.; Strack, O.L. A Discrete Numerical Model for Granular Assemblies. *Geotechnique* **1979**, *29*(1): 47-65; DOI: 10.1680/geot.1979.29.1.47.
[26] Bowman, E.T.; Soga, K.; Drummond, W. Particle Shape Characterization Using Fourier Descriptor Analysis. *Geotechnique* **2001**, *51*(6): 545-554; DOI: 10.1680/geot.2001.51.6.545.
[27] Cho, G.-C.; Dodds, J.; Santamarina, J.C. Particle Shape Effects on Packing Density, Stiffness, and Strength: Natural and Crushed Sands. *J. Geotech. Geoenviron.* **2006**, *132*(5): 591-602; DOI: 10.1061/(ASCE)1090-0241(2006)132:5(591).
[28] Ashmawy, A.K.; Sukumaran, B.; Hoang, A.V. Evaluating the Influence of Particle Shape on Liquefaction Behavior Using Discrete Element Method. *Proc. 13th Int. Offshore Polar Engineering Conf.*, Honolulu, Hawaii, USA, **2003**.
[29] Taghavi, R. Automatic Clump Generation Based on Mid-surface. *Proc.* 2nd *Int. FLAC/DEM Symp*., Melbourne, Australia, **2011**.
[30] Cavendish, J.C.; Field, D.A.; Frey, W.H. An Approach to Automatic Three Dimensional Finite-Element Mesh Generation. *Int. J. Numer. Meth. Eng.* **1985**, *8*: 329-347; DOI: 10.1002/nme.1620210210.
[31] Kim, J.H.; Kim, H.G.; Lee, B.C.; Im, S. Adaptive Mesh Generation by Bubble Packing Method. *Struct. Eng. Mech.* **2003**, *15*(1): 135-149.
[32] Hoffman, R.L. Explanations for the Cause of Shear Thickening in Concentrated Colloidal Suspensions. *J. Rheol.* **1998**, *42*(1): 111-123; DOI: 10.1122/1.550884.
[33] Stickel, J.J.; Powell, R.L. Fluid Mechanics and Rheology of Dense Suspensions. *Annu. Rev. Fluid. Mech.* **2005**, *37*(1): 129-149; DOI: 10.1146/annurev.fluid.36.050802.122132.
[34] Servais, C.; Jones, R.; Roberts, I. The Influence of Particle Size Distribution on the Processing of Food. *J. Food. Eng.* **2002**, *51*(3): 201-208; DOI: 10.1016/S0260-8774(01)00056-5.
[35] McGeary, R.K. Mechanical Packing of Spherical Particles. *J. Am. Ceram. Soc.* **1961**, *44*(10): 513-522; DOI: 10.1111/j.1151-2916.1961.tb13716.x.
[36] Lee, D.I. Packing of Spheres and Its Effect on the Viscosity of Suspensions. *J. Paint*

Techno. **1970**, *42*(550): 579-584.
[37] Metzner, A.B. Rheology of Suspensions in Polymeric Liquids. *J. Rheol.* **1985**, *29*(6): 739-775; DOI: 10.1122/1.549808.
[38] Maron, S.H.; Pierce, P.E. Application of Ree-Eyring Generalized Flow Theory to Suspensions of Spherical Particle. *J. Colloid. Sci.* **1956**, *11*(1): 80-95; DOI: 10.1016/0095-8522(56)90023-X.
[39] Eilers, H. The Viscosity-Concentration Dependence of Colloidal Systems in Organic Solvents. (in German) *Kolloid-Zeitschrift.* **1943**, *102*(2): 154-169.
[40] Krieger, I.M.; Dougherty, T.J. A Mechanism for Non-Newtonian Flow in Suspensions of Rigid Spheres. *Trans. Soc. Rheol.* **1959**, *3*(1): 137-152; DOI: 10.1122/1.548848.
[41] Chong, J.S.; Christiansen, E.B.; Baer, A.D. Rheology of Concentrated Suspensions. *J. Appl. Polym. Sci.* **1971**, *15*(8): 2007-2021; DOI: 10.1002/app.1971.070150818.
[42] Nzihou, A.; Attias, L.; Sharrock, P.; Ricard, A. A Rheological, Thermal and Mechanical Study of Bone Cement – from a Suspension to a Solid Biomaterial. *Powder Technol.* **1998**, *99*(1): 60-69; DOI: 10.1016/S0032-5910(98)00091-6.
[43] Liu, D.-M. Particle Packing and Rheological Property of Highly-concentrated Ceramic Suspensions: ϕ_m Determination and Viscosity Prediction. *J. Mater. Sci.* **2000**, *35*(21): 5503-5507; DOI: 10.1023/A:1004885432221.

Received: July 5, 2022
Revised: September 27, 2022
First published online: September 30, 2022